Global Biogeochemical Cycles

RESEARCH ARTICLE
10.1029/2018GB006049

Deep-Sea Oxygen Depletion and Ocean Carbon Sequestration During the Last Ice Age

Robert F. Anderson[1,2], Julian P. Sachs[3], Martin Q. Fleisher[1], Katherine A. Allen[4], Jimin Yu[5], Athanasios Koutavas[1,6], and Samuel L. Jaccard[7]

[1]Lamont-Doherty Earth Observatory of Columbia University, Palisades, NY, USA, [2]Department of Earth and Environmental Sciences, Columbia University, Palisades, NY, USA, [3]School of Oceanography, University of Washington, Seattle, WA, USA, [4]School of Earth and Climate Science, University of Maine, Orono, ME, USA, [5]Research School of Earth Sciences, The Australian National University, Canberra, ACT, Australia, [6]Department of Engineering and Environmental Science, College of Staten Island, City University of New York, New York, NY, USA, [7]Institute of Geological Sciences and Oeschger Centre for Climate Change Research, University of Bern, Bern, Switzerland

Key Points:
- Deep Pacific dissolved oxygen was much lower than today during the last glacial period (focusing on the interval 18,000–28,000 years BP)
- Ice age ocean storage of carbon was sufficient to explain low atmospheric CO_2 levels
- Enhanced preservation in sediments of organic compounds under low dissolved oxygen reconciles paleoproductivity proxies

Correspondence to:
R. F. Anderson,
boba@ldeo.columbia.edu

Citation:
Anderson, R. F., Sachs, J. P., Fleisher, M. Q., Allen, K. A., Yu, J., Koutavas, A., & Jaccard, S. L. (2019). Deep-sea oxygen depletion and ocean carbon sequestration during the last ice age. *Global Biogeochemical Cycles*, *33*. https://doi.org/10.1029/2018GB006049

Received 10 AUG 2018
Accepted 22 JAN 2019
Accepted article online 2 FEB 2019

Abstract Enhanced ocean carbon storage during the Pleistocene ice ages lowered atmospheric CO_2 concentrations by 80 to 100 ppm relative to interglacial levels. Leading hypotheses to explain this phenomenon invoke a greater efficiency of the ocean's biological pump, in which case carbon storage in the deep sea would have been accompanied by a corresponding reduction in dissolved oxygen. We exploit the sensitivity of organic matter preservation in marine sediments to bottom water oxygen concentration to constrain the level of dissolved oxygen in the deep central equatorial Pacific Ocean during the last glacial period (18,000–28,000 years BP) to have been within the range of 20–50 μmol/kg, much less than the modern value of ~168 μmol/kg. We further demonstrate that reduced oxygen levels characterized the water column below a depth of ~1,000 m. Converting the ice age oxygen level to an equivalent concentration of respiratory CO_2, and extrapolating globally, we estimate that deep-sea CO_2 storage during the last ice age exceeded modern values by as much as 850 Pg C, sufficient to balance the loss of carbon from the atmosphere (~200 Pg C) and from the terrestrial biosphere (~300–600 Pg C). In addition, recognizing the enhanced preservation of organic matter in ice age sediments of the deep Pacific Ocean helps reconcile previously unexplained inconsistencies among different geochemical and micropaleontological proxy records used to assess past changes in biological productivity of the ocean.

Plain Language Summary Carbon dioxide (CO_2) in Earth's atmosphere was lower during cold glacial periods of the last 800,000 years than during warm interglacial periods, by an amount equivalent to about one third of the preindustrial CO_2 content of the atmosphere. It is thought that the ocean absorbed the CO_2 missing from the atmosphere, but determining where and how the CO_2 was stored in the ocean has remained a challenge. Photosynthesis in the surface ocean converts CO_2 to organic matter, a portion of which sinks into the deep sea, where it is subsequently converted back to CO_2 by respiration of the organisms that consume the organic matter. Stimulation of the biological uptake of CO_2 in surface water, inhibition of the physical processes that raise deep waters back to the surface where they exchange gases with the atmosphere, or any combination of the two would enhance the storage of CO_2 in the deep ocean while also reducing the concentration there of dissolved oxygen. Here we show that the oxygen concentration in deep waters of the Pacific Ocean was much lower during the last glacial period than today. The difference is sufficient to accommodate the CO_2 removed from the atmosphere during the ice ages.

1. Introduction

Carbon was transferred to the ocean from the terrestrial biosphere as well as from the atmosphere during late Pleistocene ice ages (Broecker, 1982) when atmospheric CO_2 levels fell by 80–100 ppm relative to warm interglacials (Lüthi et al., 2008). Lower ice age CO_2 relative to preindustrial levels could have been influenced by a number of factors including greater ocean alkalinity, greater strength of the ocean's soft-tissue biological pump (larger inventory of ocean nutrients), greater efficiency of the biological pump (more complete biological utilization of nutrients mixed to the ocean surface), greater ocean density stratification (which reduces the evasion of respiratory CO_2 stored in the deep ocean), and greater sea ice cover in regions of deep water formation (which, like stratification, inhibits the release of CO_2 from the deep sea), in addition to the greater solubility of CO_2 in the colder ice age ocean (Archer et al., 2000; Broecker, 1982; Sigman &

Boyle, 2000; Stephens & Keeling, 2000). However, the specific contribution by each of these factors to lowering ice age CO_2 remains unresolved.

Any combination of conditions that would lower atmospheric CO_2 via an increase in the strength or the efficiency of the biological pump would lower the inventory of dissolved oxygen (DO) in the deep sea in proportion to the amount of additional respiratory CO_2 stored (Broecker, 1982; Galbraith & Jaccard, 2015; Sigman et al., 2010). Consequently, deep-ocean DO has long been recognized as the principal variable which, if reconstructed accurately, would enable investigators to quantify the portion of ice age lowering of atmospheric CO_2 attributable to enhanced storage of respiratory CO_2 in the deep sea (Boyle, 1990; Sigman et al., 2010).

A variety of independent proxy evidence indicates lower DO concentrations in the deep ocean during glacial periods. Relevant findings include deglacial peaks of MnO_2 in deep-sea sediments (Mangini et al., 1990), mineralogy of hydrothermally derived metalliferous sediments (Mills et al., 2010), empirical relationships between DO and radiocarbon ventilation age (Sarnthein et al., 2013), the difference between carbon isotopic composition of epifaunal and infaunal benthic foraminifera (Gottschalk, Skinner, et al., 2016; Hoogakker et al., 2015, 2018; Umling & Thunell, 2018), I/Ca ratios of foraminiferal calcite (Lu et al., 2016), loss of redox-sensitive magnetic minerals from deep-sea sediments (Korff et al., 2016), and the paired use of geochemical proxies for sediment redox state and for the rain rate of organic carbon delivered to the sea bed (Bradtmiller et al., 2010; Francois et al., 1997; Jaccard et al., 2009). Although the reduced deep-sea oxygenation during Pleistocene ice ages is supported by every approach employed to date, these methods are qualitative (Galbraith & Jaccard, 2015; Jaccard et al., 2014; Jaccard & Galbraith, 2012) and, in the case that benthic foraminifera are used whose depth habitat may change from epifaunal to infaunal, derive quantitative estimates of ice age DO levels with large uncertainties (Gottschalk, Skinner, et al., 2016; Gottschalk, Vázquez Riveiros, et al., 2016).

Our approach is to exploit the sensitivity of organic compound preservation in deep-sea sediments to oxygen concentration in the overlying bottom water (BWO). Exposure time to dissolved molecular oxygen is the primary variable regulating the preservation of organic matter (OM) in marine sediments (Hartnett et al., 1998). Since other factors such as sediment burial rate, sorption to mineral surfaces, and macrobenthic community structure also influence OM preservation (Arndt et al., 2013; Burdige, 2007), there is no simple relationship between BWO and the degree to which organic compounds are preserved in marine sediments. Nevertheless, empirical studies of OM preservation across a range of BWO levels in the Arabian Sea find enhanced preservation of as much as an order of magnitude when BWO levels fall below a threshold ranging between 20 and 50 μmol/kg (Cowie et al., 2014; Keil & Cowie, 1999; Koho et al., 2013; Rodrigo-Gámiz et al., 2016).

In the sections that follow we first present evidence for enhanced preservation of algal lipid biomarkers in sediments deposited during the last glacial period (LGP), emphasizing here the time interval between 18,000 and 28,000 years BP, at two sites in the central equatorial Pacific Ocean (CEP). Preservation of these compounds constrains BWO at these sites during the LGP to have been within the range identified above. We then interpret the pattern of lipid biomarker accumulation at sites covering a range of water depths in the eastern equatorial Pacific Ocean (EEP) to indicate that ice age oxygen concentrations were lower than at present at all depths greater than ~1,000 m. Lastly, we build upon these results to produce the complete dissolved inorganic carbon system for deep Pacific water during the last ice age and further argue that these findings help reconcile apparent inconsistencies in previously published paleoproductivity records from the equatorial Pacific Ocean.

2. Materials and Methods

Concentrations and burial rates of organic compounds in marine sediments are regulated by their biological production in surface waters as well as by their preservation at the seabed, so it is necessary to constrain past changes in production to infer changes in preservation from records of organic compound accumulation. We use the preserved fluxes of biogenic opal and of nonlithogenic (or excess) barium (xsBa) as inorganic indicators of past changes in biological productivity at two sites in the CEP (TT013-PC18 and TT013-PC72; Figure 1 and Table 1). Opal is composed mainly of the frustules of diatoms, phytoplankton that produce much of the

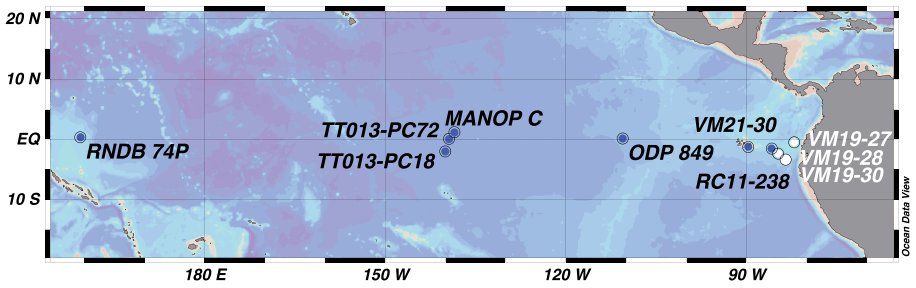

Figure 1. Equatorial Pacific sediment cores discussed in this paper. Location details are provided in Table 1. Figure prepared using Ocean Data View (http://odv.awi.de/).

carbon exported from the surface ocean (Boyd & Trull, 2007; Buesseler et al., 2007), while xsBa (barite, $BaSO_4$) microcrystals are produced primarily in the thermocline within decomposing organic aggregates (e.g., Ganeshram et al., 2003). Barite is perhaps the best calibrated and most reliable inorganic indicator for past changes in the flux of organic carbon to the deep sea in pelagic environments (Hernandez-Sanchez et al., 2011).

In addition to our new results from the CEP, we use previously published results from the EEP to define the depth interval over which organic compounds experienced enhanced preservation during the LGP. Downcore records of C_{37} alkenone concentrations in five cores from the EEP (VM21-30, VM19-27, RC11-238, VM19-28, and VM19-30; Figure 1 and Table 1) are from Koutavas and Sachs (2008).

2.1. Age Models

Published age models were used for each core (references are presented in Table 1). In addition, we systematically assign an age of 5,000 years to surfacemost sediments of CEP cores to reflect the mean age of the bioturbated mixed layer for an average mixed layer depth of 10 cm and a sediment accumulation rate of 2 cm/kyr. The assumption of a homogeneous age within the bioturbated mixed layer may not be strictly valid. However, small errors that may be introduced by this assumption do not alter our interpretation, which relies primarily on interpreting the contrasting fluxes of organic and inorganic constituents between the LGP and the postglacial period, after ~15 ka.

2.2. Opal and Excess Barium

Biogenic opal was quantified following alkaline extraction and molybdate-blue spectrophotometry using the method of Mortlock and Froelich (1989). Opal data for PC72 have been presented previously, most recently by Hayes et al. (2011) and by Winckler et al. (2016). Opal data for TT013-PC18 and TT013-MC19 are reported here for the first time. Barium concentrations in TT013-PC72 and in TT013-PC18 were taken from Murray

Table 1
Location of Cores Discussed in This Paper and Source of Stratigraphic Age Control

Core	Latitude	Longitude	Water depth (m)	Age control	References for age models
VM19-30PC	−3.383	−83.517	3,091	oxygen isotope stratigraphy	1
VM19-28PC	−2.3667	−84.65	2,720	oxygen isotope stratigraphy	2
VM19-27PC	−0.4667	−82.0667	1,373	oxygen isotope stratigraphy	3
VM21-30PC	−1.2167	−89.6833	617	^{14}C	4
RC11-238PC	−1.517	−85.817	2,573	^{14}C	4
TT013-72PC	0.1137	−139.4015	4,298	^{14}C and oxygen isotope stratigraphy	5, 6
TT013-18PC	−1.8395	−139.7137	4,354	^{14}C and oxygen isotope stratigraphy	5, 6
TT013-19MC	−1.8680	−139.7157	4,354	^{14}C	6
ODP 849	0.18333	−110.5667	3,851	oxygen isotope stratigraphy	7
RNDB 74P	0.3333	159.3667	2,547	oxygen isotope stratigraphy	8
MANOP C	0.878	−138.955	4,287	oxygen isotope stratigraphy	9

Note. References for age models: 1, Shackleton et al. (1983); 2, Martinson et al. (1987); 3, Lyle et al. (2002); 4, Koutavas and Lynch-Stieglitz (2003); 5, Murray et al. (2000); 6, R. F. Anderson et al. (2008); 7, Mix et al. (1995); 8, Perks et al. (2002); 9, Lyle et al. (1988).

et al. (2000, 2012). Nonlithogenic barium (xsBa) was calculated by slightly different approaches for the two cores. For PC72 xsBa was calculated using measured total Ba and Fe concentrations (Murray et al., 2012), assuming that all Fe is lithogenic and using the average upper continental crust Ba/Fe weight ratio of 0.01615 (Rudnick & Gao, 2003). The maximum correction was 2.1% of the total Ba. For PC18 xsBa was calculated using measured total Ba and Ti concentrations (Murray et al., 2000), because Fe data were not reported for this core, assuming that all Ti is lithogenic and using the average upper continental crust Ba/Ti weight ratio of 0.163 (Rudnick & Gao, 2003). The maximum correction was 1.5% of the total Ba. Given the small magnitude of the correction for lithogenic Ba, any systematic difference between these approaches is too small to affect our interpretation of the xsBa fluxes.

Excess barium and biogenic opal are each sensitive to variable preservation. However, the factors affecting the preservation of barite (mainly intense sulfate reduction) and the preservation of opal (in the deep sea, where temperatures are always cold, the main factor affecting opal preservation is sediment accumulation rate; Sayles et al., 2001) are unrelated to one another. Therefore, we infer that if we find similar patterns in the accumulation of opal and of xsBa then the only reasonable interpretation of our results is that fluxes of both opal and of xsBa reflect past changes in export production (Winckler et al., 2016).

Although barite tends to dissolve under conditions of intense sulfate reduction, the reducing conditions in places where this has been found (e.g., Riedinger et al., 2006; Torres et al., 1996) are much more extreme than the conditions that likely occurred in the CEP. For example, sediments at the continental margin sites off Namibia where Riedinger et al. (2006) identified barite dissolution contain 4% to 6% by weight organic carbon. By contrast, CEP sediments sampled during the TT013 cruise (near the cores we studied) contain 0.1% to 0.3% by weight organic carbon (data are archived at http://usjgofs.whoi.edu/jg/serv/jgofs/eqpac/tt013/chemistry_sed.html1%7Bdir=usjgofs.whoi.edu/jg/dir/jgofs/eqpac/tt013/,info=usjgofs.whoi.edu:80/jg/info/jgofs/eqpac/tt013/chemistry_sed%7D). Barite dissolution in the cores studied by Riedinger et al. (2006) occurred below the sulfate-methane boundary, that is, below the depth of complete sulfate reduction. It is unlikely that sulfate would ever have been depleted in CEP sediments with their low organic carbon contents. Even in the organic-rich Namibian margin sediments, barite dissolution occurs at a depth of 3 to 6 m, depending on the core site. Our records from the CEP are developed entirely from the uppermost meter of sediment, that is, well above the depth where barite dissolution occurs even in sediments with more than an order of magnitude greater organic carbon concentrations. Therefore, given that we analyzed sediments with an order of magnitude less organic carbon than at sites where barite dissolution has been reported, and that we are analyzing sediments from much shallower subbottom depth, it is safe to conclude that barite dissolution has not compromised our records. Furthermore, as shown in previous studies (Riedinger et al., 2006; Torres et al., 1996), the barite dissolved at depth later precipitates in shallower sediments after the mobilized Ba ions diffuse upward and encounter higher levels of dissolved sulfate ions, creating a well-defined peak in the sediment Ba concentration profile. As shown in our results below, we find no evidence for such barite fronts that would indicate diagenetic mobilization at depth. Consequently, one can be confident that the excess Ba records shown here have not been compromised by barite dissolution caused by sulfate reduction.

2.3. Uranium and Thorium

Uranium and thorium isotopes were measured using multiple methods over the course of nearly two decades during which the CEP cores were studied for various projects, including isotope-dilution alpha spectrometry (Lao et al., 1993) and isotope dilution inductively coupled plasma mass spectrometry (Chase et al., 2003; Fleisher & Anderson, 2003). Concentrations of unsupported ^{230}Th were derived by subtracting from the total (measured) ^{230}Th concentration the amount supported by uranium contained within lithogenic minerals and the ^{230}Th produced by decay of authigenic U (Lao et al., 1993). These corrections are small in carbonate-rich equatorial Pacific sediments (<3% each throughout the last glacial cycle for the TT013 cores), so the uncertainty introduced by these corrections represents a small component of the overall analytical uncertainty in determining initial (decay corrected) unsupported ^{230}Th concentrations (xs^{230}Th$_o$, 2% to 4%, 1 sigma), which results primarily from counting statistics. Uranium and Th data for PC72 have been presented previously in several papers, most recently by Hayes et al. (2011) and by Winckler et al. (2016). Uranium and Th data for PC18 and MC19 were reported previously by R. F. Anderson et al. (2006, 2008).

2.4. ^{230}Th-Normalized Accumulation Rates

Preserved fluxes of sedimentary constituents (xsBa, opal, organic compounds) were evaluated for the two CEP cores and for three of the five EEP cores using the ^{230}Th-normalization approach (Francois et al., 2004). This method builds upon the principle that the regional average delivery of unsupported ^{230}Th to marine sediments must be in mass balance with its known rate of production by radioactive decay of dissolved ^{234}U in the overlying water column (P_{230}). With the assumption that the flux of ^{230}Th to sediments (F_{230}) is equal to P_{230}, one can estimate the flux of any sedimentary constituent "*i*" from its measured concentration (C_i) as $F_i = (C_i/\mathrm{xs}^{230}\mathrm{Th_o}) * P_{230}$. This approach makes a necessary correction for the redistribution of sediments by deep-sea currents (syndepositional sediment focusing), and it is relatively insensitive to errors of as much as a few thousand years in the age model. Although questions have been raised concerning the assumptions inherent in this method, these questions have been addressed using a variety of approaches (R. F. Anderson et al., 2008; Costa & McManus, 2017; Francois et al., 2007; Mitchell & Huthnance, 2013; Singh et al., 2013), so we conclude that the method provides reliable estimates of the preserved fluxes of sedimentary constituents corrected for sediment focusing. Furthermore, our application of $^{230}\mathrm{Th_{xs}}$-normalized accumulation rates is limited to proxies in the fine fraction of the sediments, which is not sensitive to the reported fractionation of the coarse (carbonate) fraction during sediment redistribution (Lyle et al., 2014).

Calculated xsBa concentrations were interpolated onto the depths where we measured Th to derive ^{230}Th-normalized xsBa fluxes for the CEP cores. Point-to-point variability of xsBa flux is small (see section 3), so we conclude that the interpolation necessary to calculate fluxes has introduced insignificant error. Opal and lipid biomarker concentrations were determined using aliquots of homogenized sediment samples analyzed for U and Th, so interpolation was unnecessary in determining their fluxes.

2.5. Phytoplankton Lipid Biomarker Concentrations

Sedimentary concentrations of alkenones, C_{37} methyl ketones unique to coccolithophorid algae, and brassicasterol (24-methylcholesta-5,22E-dien-3β-ol), a marker produced by pennate diatoms and other taxa (Rampen et al., 2010; Volkman et al., 1998), were determined by gas chromatography with flame-ionization detection and co-injected standards, following identification by gas chromatography-mass spectrometry (Sachs & Anderson, 2003).

2.6. Calibration of Compound Preservation

A number of studies have exploited the intense oxygen minimum zone of the Arabian Sea as a natural laboratory to assess the sensitivity of OM preservation in marine sediments to BWO. These studies have examined sediments along the continental margins of Pakistan (Keil & Cowie, 1999) and of India (Cowie et al., 2014) as well as sediments on the Murray Ridge (Koho et al., 2013; Rodrigo-Gámiz et al., 2016; Sinninghe Damste et al., 2002), a topographic high in the Arabian Sea isolated from local continental erosion and the related supply of lithogenic material. These studies encompass a wide range of environmental conditions, including sixfold variability of sediment accumulation rate on the Murray Ridge (Lengger et al., 2014), variable mineral surface area (Keil & Cowie, 1999), and hydrodynamic sorting and grain size (Cowie et al., 2014). Any sensitivity of the organic carbon content of sediments to these variables was found to be much less than its sensitivity to BWO. Throughout the wide range of environmental conditions encountered at these sites, similar results were obtained in each case, showing a substantial increase in the preservation of both bulk OM and of specific organic compounds as BWO levels fall below a threshold between 20 and 50 μmol/kg. That similar findings were observed throughout these studies indicates that the oxygen sensitivity of compound preservation is robust across a broad range of environmental conditions. Consequently, one can have confidence in applying this threshold to other environments, including our study sites in the equatorial Pacific Ocean.

Of particular relevance to our equatorial Pacific study is the work of Rodrigo-Gámiz et al. (2016) who assessed the preservation of C_{37} alkenones, one of the compound classes used in our study, in a suite of cores from sites on the Murray Ridge with BWO levels ranging from 3 to 77 μmol/kg. Working within a confined spatial area far from land, the authors could assume that the rain of particulate organic compounds to the seabed was uniform among their study sites, as was the rain of lithogenic particles, supplied largely as dust, which could influence the concentration of organic compounds by variable dilution. Although the sinking flux of particulate organic compounds decreases with depth in the water column, most of the flux

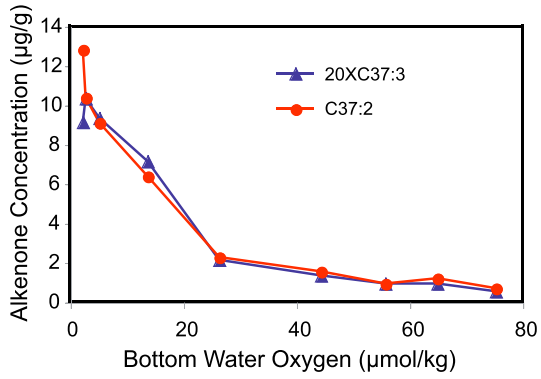

Figure 2. Alkenone concentrations in core top sediments from the Murray Ridge (from supplementary data in Rodrigo-Gámiz et al., 2016) plotted against bottom water oxygen concentration (from Koho et al., 2013). Concentrations of $C_{37:3}$ alkenones have been multiplied by 20 to place them on the same scale as the concentrations of $C_{37:2}$ alkenones. The change in slope between 20 and 40 µmol/kg represents one of the findings used to constrain a BWO range of 20–50 µmol/kg for substantially increased preservation of organic compounds under low-oxygen conditions.

attenuation occurs above 500 m, with relatively little change below 885 m (Martin et al., 1987), the depth of the shallowest core examined in the Murray Ridge study (Lengger et al., 2014). Ruling out production, dilution, and depth as factors affecting the concentration of lipid biomarkers, the remaining factor that would influence core-to-core variability of C_{37} alkenone concentration is preservation.

Concentrations of C_{37} alkenones in surface sediments were found to increase systematically by an order of magnitude as BWO decreased from 77 to 3 µmol/kg (Figure 2). Sediment accumulation rates at the three shallowest sites (lowest BWO; 13.4, 4.0, and 2.2 cm/kyr) span a range similar to those at the three deepest sites with the highest BWO (2.6, 2.6, and 8.3 cm/kyr; Lengger et al., 2014). The systematic decrease in alkenone concentration in Figure 2 indicates that alkenone preservation is far more sensitive to BWO than to sediment accumulation rate. The greatest change in the slope of the relationship between alkenone concentration in surface sediments and BWO was observed at an oxygen concentration between 20 and 40 µmol/kg (Figure 2). This is consistent with earlier work reporting that the rate constant for OM degradation at these sites decreased by a factor of 3 across this same range of BWO levels (see Figure 3 in Koho et al., 2013). We use these results together with similar findings from the other sites in the Arabian Sea, cited above, to estimate a BWO threshold for increased lipid biomarker preservation of 20–50 µmol/kg.

The data shown in Figure 2 reflect the relative preservation of C_{37} alkenones under conditions where all core sites receive the same supply of particulate constituents (clay, opal, $CaCO_3$, and biomarker compounds). Bottom water oxygen concentrations at other locations, with different input rates of sedimentary constituents, cannot be inferred directly from measured C_{37} alkenone concentrations using the relationship between C_{37} alkenone concentration and BWO in Figure 2.

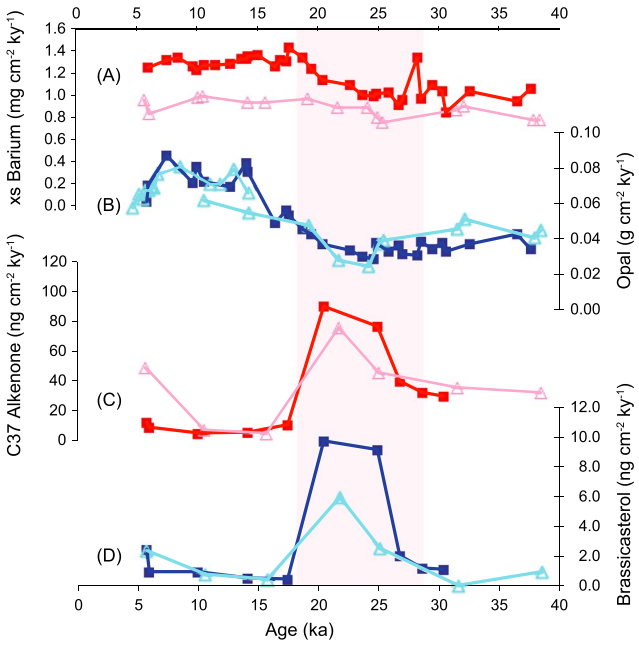

Figure 3. ^{230}Th-normalized fluxes of biogenic constituents in central equatorial Pacific cores TT013-PC72 (solid squares, darker lines) and TT013-PC18 (open triangles). The shaded region represents the last glacial period (defined here as 18–28 ka). (a) Nonlithogenic (xs) barium, (b) biogenic opal, (c) C_{37} alkenones, and (d) brassicasterol. In (b) greater sampling resolution for the late deglacial and Holocene opal flux is provided by splicing data from a multicore (MC19) collected near the location of the piston core (PC18) at 2°S (locations in Table 1).

3. Results

In both CEP cores we find lower preserved fluxes of opal and xsBa during the LGP than during the postglacial period (Figures 3a and 3b), consistent with findings throughout the CEP indicating that export production during the last ice age was less than during the Holocene (Costa et al., 2017). In contrast to these inorganic proxies, the preserved fluxes of C_{37} alkenones, produced by coccolithophoridae (Volkman et al., 1998) and of 24-methylcholesta-5,22E-dien-3β-ol (brassicasterol), produced by pennate diatoms (Rampen et al., 2010) and other taxa (Volkman et al., 1998), during the LGP are as much as an order of magnitude greater than during the postglacial period (Figures 3c and 3d). Higher lipid fluxes in bioturbated surface sediments, with an average age of 5,000 years, reflect incorporation of recently deposited material and incomplete loss of compounds during early diagenesis (Prahl et al., 1989), so these data are excluded from our interpretation of changes in BWO.

Alkenone concentrations for the five EEP cores (Figure 4b) were published previously (Koutavas & Sachs, 2008). Uranium and thorium data are available for three of these cores: VM19-30, RC11-238, and VM19-27 from Hayes et al. (2011), Bradtmiller et al. (2010), and this work, respectively. ^{230}Th-normalized mass fluxes are relatively constant over the past 30,000 years in each of these cores (not shown). Consequently, the temporal pattern of alkenone concentration in each of these cores reflects the preserved alkenone flux (Figure 5). We assume that this condition

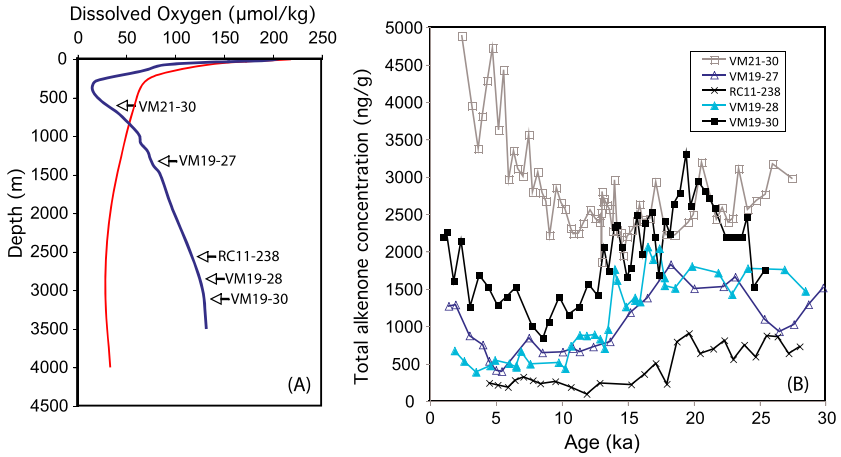

Figure 4. Concentrations of C_{37} alkenones in five eastern equatorial Pacific cores (locations in Figure 1 and Table 1) from sites spanning a range of depths and bottom water oxygen concentrations. (a) A representative dissolved oxygen profile from the eastern equatorial Pacific Ocean (2.5°S, 85.5°W, extracted from gridded data in the World Ocean Atlas 09, Garcia et al., 2010, blue curve), with each core plotted at its collection depth next to the modern oxygen profile. (b) Concentrations of C_{37} alkenones (data from Koutavas & Sachs, 2008) in sediments deposited over the past 30,000 years at the five locations (cores are identified in the legend). Alkenone concentrations reveal the same pattern as their preserved flux in three cores for which ^{230}Th data are available (Figure 5), so the alkenone concentrations shown here are representative of their accumulation rates. The red curve in (a) with lower deep water dissolved oxygen concentrations is a plausible equatorial Pacific dissolved oxygen profile for the last glacial period constrained by preservation of organic compounds (see text for details).

also applies to the two cores for which ^{230}Th data do not exist, and thus we use alkenone concentration (Figure 4b) rather than flux to assess the depth dependence of time-varying changes in alkenone preservation.

4. Discussion

The preserved fluxes of opal and of xsBa during the LGP were lower than during the postglacial record (Figures 3a and 3b). As these inorganic proxies represent the time-varying rain of organic carbon produced by major phytoplankton taxa, the records of lipid biomarker accumulation (Figures 3c and 3d) indicate that preservation of organic compounds was enhanced by about an order of magnitude in the CEP during the LGP.

Previous work in the CEP reported results consistent with ours. At MANOP Site C (0.878°N, 138.955°W), near the location of our TT013 cores (Figure 1 and Table 1), Prahl et al. (1989) described eightfold greater accumulation of C_{37} alkenones during the last glacial maximum compared to the Holocene, similar to our results (Figure 3c), as well as fifteenfold greater accumulation of dinosterol, a compound produced by dinoflagellates. Therefore, with similar results from three sites (TT013-PC18, TT013-PC72, and MANOP Site C) and for lipid biomarkers representing three major taxonomic groups (diatoms, prymnesiophytes, and dinoflagellates, represented by brassicasterol, C_{37} alkenones, and dinosterol, respectively), combined with widespread evidence for lower export production in the CEP during the LGP (this work, Costa et al., 2016, 2017; Winckler et al., 2016), one can be confident that the order of magnitude greater accumulation of these lipid biomarkers during the LGP reflects greater preservation of OM and not simply a shift from one dominant phytoplankton taxon to another.

Modern BWO concentrations at these CEP sites are ~168 µmol/kg (Table 2). Applying the empirical results from the Arabian Sea described above, we conclude that BWO at these locations during the LGP fell within the range 20–50 µmol/kg, 118–148 µmol/kg lower than today. To illustrate changes in apparent oxygen utilization (AOU, Table 2), carbon storage (Table 3), and in the inorganic carbon system (Table 4), we use the midpoint in the BWO range (35 µmol/kg) for calculations in the sections that follow.

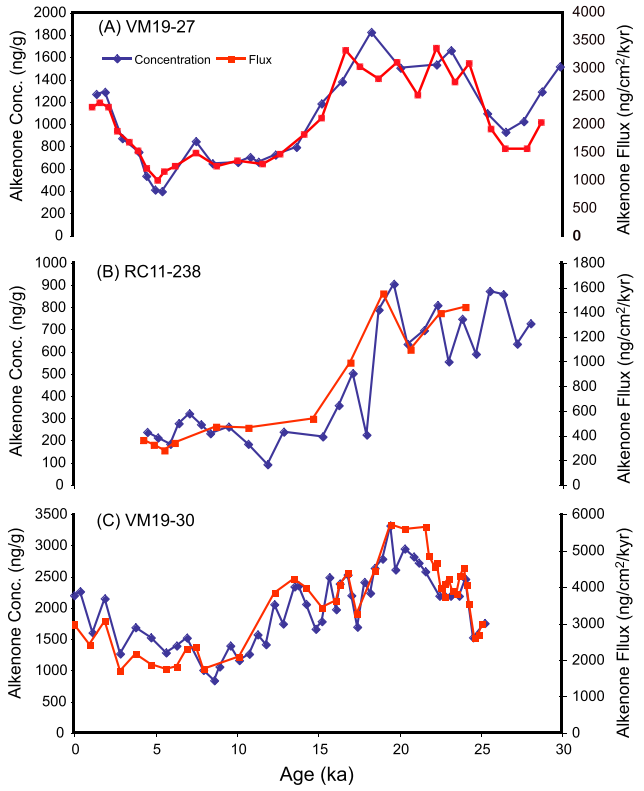

Figure 5. Concentrations and ^{230}Th-normalized fluxes of C_{37} alkenones in three eastern equatorial Pacific Ocean cores. Concentrations are plotted at ages corresponding to their original sample depths. Fluxes are calculated by interpolating alkenone concentrations onto depths of the thorium samples. Alkenone data are from Koutavas and Sachs (2008). ^{230}Th data for (c) VM19-30, (b) RC11-238, and (a) VM19-27 are from Hayes et al. (2011), Bradtmiller et al. (2010), and this work, respectively. Late Holocene (post 5 ka) increases in the flux and concentration of C_{37} alkenones reflect the progressive loss of organic material during early sediment diagenesis (Prahl et al., 1989) rather than a late Holocene decrease in BWO (increase in alkenone preservation).

4.1. Depth Distribution of Reduced Ice Age Oxygen

Evidence from a variety of indicators informs us that low-DO conditions existed throughout the deep Pacific Ocean below the thermocline during the LGP (see section 1 and reviews by Galbraith & Jaccard, 2015; Jaccard et al., 2014; Jaccard & Galbraith, 2012). Alkenone preservation in sediments from the EEP is consistent with this view. The five EEP cores used in this study (Figure 1 and Table 1) were recovered from sites bathed by nearly the full range of modern BWO (Figure 4a). These sites are in close proximity to one another and thus share a common history of sea surface temperature (Koutavas & Sachs, 2008), so we assume that the pattern of climate-related change in export production, such as might occur in response to wind-driven upwelling, and any change in the supply of lithogenic phases that may also affect the concentration of biogenic constituents, would be coherent among these sites as well. This view is supported by ^{230}Th-normalized alkenone fluxes, which map well onto the alkenone concentration patterns for three of the five sites for which ^{230}Th data are available (Figure 5). Consequently, any differences among the sites in the pattern of alkenone concentration over time is attributed to varying preservation rather than site-to-site differences in productivity (Rodrigo-Gámiz et al., 2016).

During the LGP, alkenone concentrations at the shallowest site (VM21-30) are indistinguishable from those at the deepest site (VM19-30; Figure 4b). Concentrations at these sites diverge during deglaciation (~18–10 ka) and remain consistently greater at the shallow site throughout the Holocene. Today, the shallowest site is located under a much lower BWO level than is the deepest site (Figure 4a). Using Holocene sediments as a guide, we interpret the similar alkenone concentrations during the LGP at these two sites to indicate greater alkenone preservation under reduced BWO levels at the deepest site, consistent with our results from the CEP. Greater DO concentrations at the thermocline depth of VM21-30 (Galbraith & Jaccard, 2015; Jaccard & Galbraith, 2012) may have also led to lower alkenone preservation there during the LGP than today.

Each of the other records (Figure 4b) presents a pattern of alkenone concentration that is more similar to that of VM19-30 (decreasing during deglaciation) than to that of VM21-30, indicating a general decrease in alkenone preservation through deglaciation. As for the CEP cores described above, the late-Holocene increase in alkenone concentration reflects incomplete early diagenesis of organic compounds (Prahl et al., 1989) rather than a decrease in BWO. Based on the dissimilar patterns between the shallowest core (VM21-30) and each of the other cores (Figure 4b), we

Table 2
Hydrographic Conditions Representative of ~4.2-km Depth at the Equator and 140°W for the Modern Ocean and Estimated for the Last Glacial Period

Period	Salinity	Temperature (°C)	Potential temperature (°C)	O_2 (μmol/kg)	O_2 solubility (μmol/kg)[a]	AOU (μmol/kg)[b]
Modern[c]	34.694	1.41	1.0616	168	351	183
LGP[d]	35.734	−0.59	−0.9384	35[e]	371	336

[a]The solubility of dissolved oxygen at each salinity and potential temperature is calculated according to Garcia and Gordon (1992). [b]Apparent oxygen utilization (AOU) is calculated as the difference between oxygen solubility (saturation) and in situ dissolved oxygen concentration. [c]Modern temperature, salinity (bottle salinity), potential temperature, and dissolved oxygen concentration are taken from the U.S. Joint Global Ocean Flux Study (JGOFS) data base for cruise TT012 Station 5 Cast 83 in 1992 (http://usjgofs.whoi.edu/jg/serv/jgofs/eqpac/tt012/bottle_merged.html1?sta eq 5/). [d]For the last glacial period (LGP) we apply an average increase in ocean salinity of 3% corresponding to a drop in sea level of ~120 m (Fairbanks, 1989) and a decrease in deep Pacific temperature (and potential temperature) of 2 °C (Elderfield et al., 2010). [e]The dissolved oxygen concentration during the LGP (35 μmol/kg) used to constrain AOU is the midpoint of the range of BWO values (20–50 μmol/kg) that allow for greatly increased preservation of organic matter in marine sediments (see main text for explanation).

Table 3
Tie Points Illustrating the Backward Derivation of Deep Pacific Carbonate Chemistry During the LGP as Shown in Figure 6

Graph points	Condition	$CaCO_3$ (μmol/kg)	TCO_2 (μmol/kg)	TALK (μmol/kg)	$[CO_3^{2-}]$ (μmol/kg)
1	Modern 0°, 140°W, 4.2 km		2320	2425	79
2	Modern + ice volume		2385	2498	82.8
	Mod+ice+DeltaRespCO_2		2494	2498	39.3
3	Plus respiratory HNO_3		2494	2481	34.4
4	$CaCO_3$ dissolution	109	2603	2699	79.3

Note. See the main text for details. LGP = last glacial period.

infer that the boundary between water masses with greater DO concentrations during the LGP and those with lower DO levels was situated between the depths of VM21-30 and VM19-27 (617 and 1,373 m, respectively), consistent with the LGP oxygen distribution inferred using other proxies (Galbraith & Jaccard, 2015; Jaccard et al., 2014; Jaccard & Galbraith, 2012). Greater water column density stratification above 1,000 m (Bova et al., 2015) during the LGP likely influenced the evolving pattern of DO distribution (Sigman et al., 2010), although other factors may have contributed as well.

Barium has not been measured at any of the EEP sites for which we present alkenone data (Figure 4b). Among these five cores, opal fluxes and unsupported $^{231}Pa/^{230}Th$ ratios, also considered a paleoproductivity proxy, have been reported for VM19-30 and RC11-238, both of which have slightly lower values during the LGP than during the Holocene (Bradtmiller et al., 2006). This fits into the general pattern of lower productivity during the LGP in the EEP described by Costa et al. (2017). Declining concentrations and fluxes of alkenones during deglaciation for the four deeper EEP cores across an interval of generally increasing productivity supports the interpretation of greater preservation of alkenones during the LGP for each of cores except the shallowest (VM21-30).

Assuming that DO levels throughout the equatorial Pacific were similarly affected during the LGP, we present a plausible ice age DO profile (red curve in Figure 4a) for the equatorial Pacific Ocean. The LGP oxygen profile is constructed with four constraints: (1) surface waters in equilibrium with the atmosphere were not very different from modern conditions; (2) DO at the depth of VM21-30 was greater during the LGP than today (see above); (3) the crossover point where DO during the LGP was approximately the same as today was situated between the depths of VM21-30 and VM19-37, with DO less than modern conditions at all greater depths; and (4) the DO concentration was 35 μmol/kg at 4.2 km in the central equatorial Pacific (see above). It is further assumed that the deep Pacific Ocean was ventilated from the Southern Ocean at abyssal depths during the LGP (Elderfield et al., 2010; Hall et al., 2001), as it is today, so that BWO at ~4 km were slightly greater than at depths of ~3 km corresponding to the southward return flow, as is the case in the modern ocean.

Table 4
Salinity-Normalized (S_N) TCO_2 and TALK for Modern and LGP Conditions for Bottom Water Overlying Our Core Sites in the CEP (Equator, 140°W), Together With the Absolute and Relative Change in Each

Period/Variable	S_N TCO_2 (μmol/kg)	S_N TALK (μmol/kg)
Modern	2,340	2,446
LGP	2,550	2,644
Delta-absolute	209	198
Delta-%	8.9%	8.1%

Note. Normalization is to $S = 35$ on the Practical Salinity Scale of 1978. TCO_2 = total dissolved inorganic carbon; TALK = total alkalinity; LGP = last glacial period; CEP = central equatorial Pacific Ocean; Delta = difference between LGP and Modern.

4.2. Implications for Carbon Storage

Respiratory CO_2 is related to AOU, which is generally calculated assuming that deep water forms at the sea surface with DO in thermodynamic equilibrium with the atmosphere at the temperature (T) and salinity (S) of the water mass. Beginning with T and S measured at the TT013 core sites (Table 2), and allowing for LGP conditions of 3% greater S due to freshwater storage in continental ice sheets and a 2 °C lower T (Elderfield et al., 2010), together with the measured historical BWO (168 μmol/kg, Table 2), we calculate an AOU of bottom water during the LGP of 336 (range 321–351) μmol/kg, or 153 (range 138–168) μmol/kg greater than today (Table 2). Using a respiratory quotient (moles of O_2 consumed per mole of CO_2 produced) of 1.414 (L. A. Anderson, 1995), we conclude that the total respiratory CO_2 in equatorial Pacific bottom water during the LGP was 108 (range 98–119) μmol/kg greater than today.

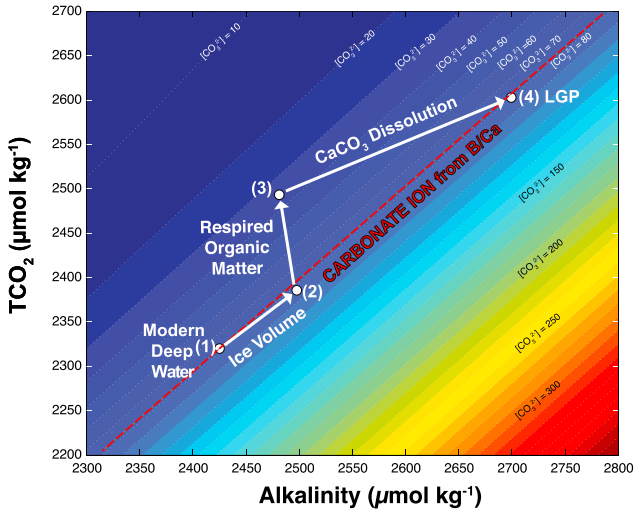

Figure 6. Backward trajectory of central equatorial Pacific bottom water carbonate chemistry from modern measured values to values inferred for bottom water during the last glacial period (Table 3). The principal changes reflect the 3% reduction in ocean volume during the LGP when freshwater was locked up in continental ice sheets (ice volume), the greater concentration of respiratory CO_2 in bottom water during the LGP (respired organic matter, this work), and the requirement that substantial dissolution of $CaCO_3$ allowed the dissolved carbonate ion concentration during the LGP at these locations to have been not detectably different from modern values (D. M. Anderson & Archer, 2002; Yu et al., 2013). Carbonate ion contours (colored lines) were calculated using LGP temperature and salinity (Table 2). LGP = last glacial period.

Extrapolating to the global ocean is tenuous with limited data, but to illustrate the potential scale of enhanced CO_2 storage during the LGP, we note that most of the deep Pacific (Figure 4a and Jaccard & Galbraith, 2012), Atlantic (Hoogakker et al., 2015) and Southern Oceans (Francois et al., 1997; Gottschalk, Skinner, et al., 2016; Jaccard et al., 2016) held substantially more respiratory CO_2 (i.e., had lower DO) during the LGP (see also de la Fuente et al., 2017; Sarnthein et al., 2013; Skinner et al., 2015; Skinner et al., 2017). Partially offsetting this enhanced deep-sea CO_2 storage, the surface ocean, in equilibrium with atmospheric CO_2 at 180 to 200 ppm, would have held less dissolved carbon than today. However, as noted above, this condition was likely restricted to the upper kilometer of the water column, above the level of enhanced stratification. Thus, for illustration we assume that half the ocean volume during the LGP held 108 μmol/kg more respiratory CO_2 relative to modern conditions, as we derive for the deep Pacific Ocean. In this case, the global ocean inventory of respiratory CO_2 during the LGP would have been ~850 Pg C greater than today, sufficient to accommodate 200 Pg C removed from the atmosphere and the carbon lost from the terrestrial biosphere (330–694 Pg C; Peterson et al., 2014). The uncertainty in this estimate is quite large (see section 4.6), but our finding is consistent with other estimates reached by a variety of independent approaches (Jaccard et al., 2009; Sarnthein et al., 2013; Schmittner & Somes, 2016; Skinner et al., 2015).

4.3. Ice Age Inorganic Carbon System of the Deep Pacific Ocean

Building on our estimate of respiratory CO_2 in the deep Pacific Ocean during the LGP, and noting that the dissolved carbonate ion concentration, $[CO_3^{2-}]$, in deep Indo-Pacific water was not significantly different from its modern value, as determined using two independent approaches (D. M. Anderson & Archer, 2002; Yu et al., 2013), we derive the complete CO_2 system for deep Pacific water during the LGP (Figure 6 and Table 3). Given the much greater concentration of respiratory CO_2 during the LGP, described above, the existence of $[CO_3^{2-}]$ similar to modern values implies dissolution of a substantial amount of $CaCO_3$ to raise the total alkalinity (TALK) of seawater, as expected from the principles of carbonate compensation (Boyle, 1988; Broecker & Peng, 1987) and as has been inferred independently from studies of the $CaCO_3$ content of equatorial Pacific sediments (e.g., R. F. Anderson et al., 2008; Broecker & Sanyal, 1997).

Derivation of LGP carbonate system parameters was carried out in a sequence of steps beginning with modern conditions. Point 1 (modern deep water, Table 3 and Figure 6) represents modern conditions, using *T* and *S* from Table 2 together with average TCO_2 (total dissolved inorganic carbon) and TALK extracted from the GLODAP data base (http://cdiac.ornl.gov/oceans/glodap/) between 5°N and 4°S, 135°W and 140°W, 4.2 and 4.5 km, using Ocean Data View (http://odv.awi.de/). Carbonate ion concentration was calculated using CO2SYS v2.1 (http://cdiac.ornl.gov/oceans/co2rprt.html) using K_1 and K_2 from Mehrbach et al. (1973), as refit by Dickson and Millero (1987), the seawater pH scale (mol/kg-SW), $KHSO_4$ from Dickson (1990), and total boron from Uppstrom (1974). All carbonate ion contours in Figure 6 were calculated assuming LGP temperature and salinity values from Table 2 and a pressure of 4,170 dbar (modern water depth minus 120 m of sea level drop). The influence of glacial-interglacial temperature, salinity, and pressure changes on calculated carbonate ion are minimal, with a combined average effect of 1 μmol/kg and a maximum effect of 2 μmol/kg. Therefore, it is reasonable to plot modern and LGP estimates on the same contours.

Point 2 corrects for the 3% lower ocean volume at the peak of the last ice age, assuming that nonrespiratory (preformed) CO_2 and TALK both increase by 3%. Nonrespiratory CO_2 is calculated as $TCO_2 - AOU/RQ$, where RQ is the respiratory quotient (assumed here to be 1.414; L. A. Anderson, 1995). Temperature and salinity for the LGP (Table 2) were used for these calculations. The slope (unitless) of the vector from Point 1 to Point 2 is 0.890.

The impact on the CO_2 system of increasing AOU from 183 to 336 μmol/kg (Table 2) is evaluated in two steps. First, the total respiratory CO_2 (AOU/RQ) for the LGP is added to the ocean-volume-corrected nonrespiratory CO_2, calculated as described in the paragraph immediately above. Then an additional adjustment is made to the ocean-volume-corrected TALK for the loss of alkalinity by addition of HNO_3 from respiration, assuming complete oxidation of organic N delivered to the deep sea with an organic C/N molar ratio of 106/16 (Redfield, 1958). This leads to Point 3 where the slope of the vector from Point 2 to Point 3 is −6.41.

Lastly, Point 4 (LGP conditions following $CaCO_3$ dissolution) is reached by adding TALK and TCO_2 in a 2:1 ratio to represent $CaCO_3$ dissolution until sufficient $CaCO_3$ has dissolved to raise the carbonate ion concentration back to the initial value, consistent with reconstructions for the LGP (D. M. Anderson & Archer, 2002; Yu et al., 2013). The slope of the vector from Point 3 to Point 4 is 0.5.

Dissolution of $CaCO_3$ raised the ocean's alkalinity (8.1% increase in salinity-normalized [S_N] TALK, Table 4), thereby contributing to the ice age drawdown of atmospheric CO_2 (Archer et al., 2000; Archer & Maier-Reimer, 1994; Sigman & Boyle, 2000). The additional CO_2 drawdown attributable to this carbonate compensation effect has been calculated to fall in the range of 15–30% depending on ocean circulation and other boundary conditions (Hain et al., 2010; Kobayashi & Oka, 2018; Omta et al., 2018). Furthermore, the greater S_N TALK during the LGP should be taken into account when past changes in the partial pressure of CO_2 and other carbon system parameters are calculated by combining information from boron isotope proxies for pH with an assumed value of S_N TALK (e.g., Honisch et al., 2009; Martinez-Boti et al., 2015; Palmer & Pearson, 2003; Rae et al., 2018).

These findings will be refined as additional estimates for BWO and carbonate ion concentration become available. Until then, our findings provide useful targets for modeling of the ocean carbon system during the last ice age.

4.4. Implications for Reconstructing Paleoproductivity

Beyond providing a foundation for more sophisticated models of the ice age global carbon budget, our findings help resolve long-standing questions in paleoceanography. For example, recognizing the enhanced preservation of organic carbon under low BWO of the ice age equatorial Pacific Ocean reconciles the inconsistency between estimates of paleoproductivity based on benthic foraminifera assemblages and inorganic proxies, which are interpreted to indicate similar or lower levels of productivity during the LGP, and those based on organic carbon accumulation, which have been interpreted to indicate greater ice age productivity (e.g., Costa et al., 2017; Loubere, 1999; Lyle, 1988; Lyle et al., 1988; Pedersen, 1983; Sarnthein et al., 1988; Winckler et al., 2016).

Our findings also offer a new interpretation of combustion oxygen demand (COD), a yet overlooked technique to measure the total amount of organic carbon and reduced inorganic compounds in marine sediments (Perks et al., 2002; Perks & Keeling, 1998). Whereas COD was originally interpreted as an indicator of paleoproductivity (Perks & Keeling, 1998), the greater measured COD in western Pacific sediments (RNDB 74P, Figure 1) than in the east (ODP 849), during both glacial and interglacial periods, was noted to be at odds with the modern pattern of productivity, which is greater in the east (Perks et al., 2002). Perks and coworkers (Perks et al., 2002; Perks & Keeling, 1998) also found the temporal pattern of COD variability to be in phase at the two sites (higher during glacial periods), which is unexpected because productivity in the eastern and western equatorial Pacific regions has varied historically in an opposing sense, reflecting changes in the tilt of the thermocline (nutricline) that influences the local delivery of nutrients to the euphotic zone.

These findings make sense, however, recognizing that core RNDB 74P was collected from a shallower depth (2,547 m, Table 1), within the low-oxygen return flow of Pacific deep water, whereas the deeper eastern location of ODP 849 (3,851 m) lies within more recently ventilated bottom water bearing a greater DO content. We interpret these results to suggest that COD is more sensitive to BWO than to biological productivity. With further testing and calibration, COD combined with inorganic proxies of carbon supply, such as opal and xsBa (Figure 3), may offer a rapid means to map the deep-sea DO distribution under past climate regimes.

4.5. Internal Consistency Among Independent Approaches

Our conclusions concerning oxygen levels in the deep Pacific Ocean during the LGP were derived by applying an empirical relationship between the preservation of OM in Arabian Sea sediments and the

concentration of oxygen in the overlying bottom water (section 2.6). Although the oxygen concentrations over which preservation increased most rapidly consistently fell in the range 20–50 μmol O_2/kg under a variety of sedimentary conditions, there remains some uncertainty about extrapolating this relationship to deep equatorial Pacific sediments. It is noteworthy, therefore, that during the time this paper was in revision, Hoogakker et al. (2018) published results from the EEP that are consistent with our findings. Using the carbon isotopic composition of paired benthic foraminifera (epibenthic and infaunal; Hoogakker et al., 2015), Hoogakker et al. (2018) reported bottom water oxygen levels at the site of TR163-25 (1.65°S, 88.45°W, 2.65 km) as low as 30–50 μmol/kg during the LGP, within the range of BWO that we infer by applying the relationship between BWO and organic carbon preservation derived from studies in the Arabian Sea. While each approach involves inherent assumptions and uncertainties, the internal consistency obtained using these two very different approaches lends confidence to the shared conclusion that oxygen concentrations in the deep equatorial Pacific Ocean likely fell below 50 μmol/kg during the LGP.

4.6. Outlook for Future Developments

Although low LGP oxygen levels in the deep Pacific are supported by independent approaches, the implications for CO_2 storage depend on additional factors such as the composition of the OM respired in the deep sea and the initial concentration of DO at the time the water mass was formed. Each of these topics is addressed briefly here.

In calculating the additional CO_2 sequestered in the deep ocean during the LGP we used the respiratory quotient reported by L. A. Anderson (1995). The actual value of the RQ will vary with the composition of the OM; for example, it is much larger for lipids (RQ ~ 1.5) than for carbohydrates (RQ ~ 1.0) or proteins (intermediate values, reviewed in Chapter 6 of Sarmiento & Gruber, 2006). Recent studies have also pointed out that the elemental composition of OM varies with time and with location in the ocean (e.g., DeVries & Deutsch, 2014; Martiny, Pham, et al., 2013; Martiny, Vrugt, et al., 2013; Talarmin et al., 2016). We recognize the need for future modeling studies (e.g., DeVries, 2018; Tanioka & Matsumoto, 2017) to explore the sensitivity of CO_2 sequestration to BWO under conditions of varying OM composition.

Another concern is that bottom water formed around Antarctica may leave the sea surface with an oxygen concentration that is not entirely in equilibrium with the atmosphere. If that were the case, then it would introduce error into the calculation of AOU and, thus, in the estimated level of respiratory CO_2. Two key points need to be considered in this context. First, the level of oxygen undersaturation in newly formed bottom waters has been overestimated in some cases. This is because various authors have taken average O_2 concentration in surface waters as representative of the bottom water formed around Antarctica (e.g., Duteil et al., 2013; Ito et al., 2004). For example, Duteil et al. (2013) cite Gordon and Huber (1990) for low O_2 concentrations in surface waters of the Weddell Sea to estimate an O_2 saturation of 86% in newly formed bottom water. However, as Gordon and Huber (1990) pointed out, extrapolating O_2 concentration in surface water back in time to the first formation of sea ice gives an O_2 saturation level of 96%, much greater than the 86% assumed by Duteil et al. (2013). Furthermore, Gordon et al. (2001) showed that O_2 concentrations are much greater along the western margin of the Weddell Sea, where bottom water forms, than in the interior of the Weddell Sea, where doming of isopycnals associated with upwelling of oxygen-deficient Modified Circumpolar Deep Water prevents complete equilibration with the atmosphere, generating the low O_2 saturation values reported by Gordon and Huber (1990) and used by Duteil et al. (2013). Future studies that rely on oxygen saturation in newly formed bottom waters should be careful to use values that are representative of surface waters in coastal regions where buoyancy loss leads to bottom water formation.

Second, to the extent that surface waters that form the precursor to Antarctic Bottom Water are undersaturated in O_2 with respect to equilibrium with the atmosphere, the implications for respiration rates in the deep sea inferred from AOU are opposite those for CO_2 storage. This distinction is not necessarily intuitive so it is worthy of mention. Duteil et al. (2013) noted that respiration in the deep sea calculated using AOU may be overestimated by as much as 25%, depending on the preformed O_2 concentration assumed. While this is true, it does not mean that the amount of respiratory CO_2 stored in the deep sea is overestimated by an equivalent amount. To the contrary, exactly the opposite situation arises. Because O_2 equilibrates with the atmosphere more than an order of magnitude more rapidly than does CO_2 (Broecker & Peng, 1974), the degree of disequilibrium for CO_2 in newly formed bottom water will always be greater than for O_2. Ito and

Follows (2013) modeled this phenomenon, and for the conditions assumed in their model, they concluded that air-sea gas disequilibrium at the time of bottom water formation amplifies the storage of CO_2 in the deep sea via the biological pump by as much as 70% above that inferred from AOU. We suspect that the O_2 disequilibrium assumed by Ito and Follows (2013) may be overestimated, for the reasons outlined above. Nevertheless, the principle is sound. Therefore, if bottom water were formed during the LGP with an initial O_2 concentration well below that assumed based on saturation with the atmosphere at the salinity and potential temperature of the water, then the CO_2 storage would have been greater than inferred from multiplying AOU by the RQ as we did in forming our estimate of CO_2 storage during the LGP.

Lastly, our estimate of the additional storage of CO_2 in the deep sea during the LGP (up to 850 Pg C) encompasses the CO_2 removed from the atmosphere and most of the wide range of estimates for carbon lost from the terrestrial biosphere (Peterson et al., 2014; Peterson & Lisiecki, 2018). Oxidation of terrestrial OM on land would have released this CO_2 directly into the atmosphere. Under conditions of lower atmospheric pCO_2 during the LGP, the ocean's "solubility pump" (Sarmiento & Gruber, 2006) would not have contributed significantly to the transfer of this terrestrial CO_2 to the deep sea. Rather, deep-sea sequestration of this terrestrial CO_2 must have been achieved by increased strength or efficiency of the biological pump, consistent with our rough estimate of global lowering of the inventory of DO in the deep ocean during the LGP. Efforts to map the areas of low BWO during the LGP (Jaccard et al., 2014; Jaccard & Galbraith, 2012), combined with efforts to calibrate existing and new sedimentary proxies for oxygen, as well as efforts to model the sensitivity of CO_2 storage to varying oxygen levels, including the factors described above, will all improve the quantification of ocean CO_2 storage during the LGP and our knowledge of the processes regulating it.

5. Summary

Reduced oxygenation of deep water in the Pacific Ocean during the LGP is a robust finding. Multiple independent indicators point to lower oxygen in the deep Pacific Ocean. Preservation of phytoplankton lipid biomarkers in equatorial Pacific sediments at a depth of ~4.2 km was approximately an order of magnitude greater during the LGP compared to postglacial conditions. We interpret the greater preservation of algal lipids to indicate that LGP bottom water oxygen levels were within the range 20–50 μmol/kg, between 118 and 148 μmol/kg less than today, and that DO levels below modern values occurred at all depths below about 1,000 m. Extrapolating globally, with large uncertainty due to the paucity of data, we estimate that global ocean storage of carbon during the LGP exceeded modern levels by as much as 850 Pg C and that salinity-normalized alkalinity exceeded modern values by about 8%. Reorganization of ocean and atmospheric circulation during the termination of the last ice age released this carbon to the atmosphere, accounting for the deglacial rise in atmospheric CO_2 (R. F. Anderson et al., 2009; Denton et al., 2010; Rae et al., 2018). Given that essential information about the ocean carbon cycle and its sensitivity to climate change can be extracted using reconstructed oxygen levels, it would be worthwhile for the paleoceanographic community to organize an effort to develop more objective and quantitative proxies for paleo-oxygen (Boyle, 1990). Given the sensitivity of each proxy to multiple factors, a multiproxy approach is likely to be needed.

Acknowledgments
The authors declare no competing financial interests. Data presented in this paper are archived at the National Center for Environmental Information through their Paleoclimatology division (https://www.ncdc.noaa.gov/paleo/study/25630). Alkenone data shown in Figure 4b are also available at the website (https://www.ncdc.noaa.gov/paleo/study/25670). Several grants from the U.S. National Science Foundation supported the production of the data reported here during the course of previous studies. However, the synthesis of results presented here was carried out without directed grant support except that S. L. J. acknowledges financial support by the Swiss National Science Foundation (grants PP00P2-144811 and PP00P2-172915). This paper was much improved by comments from Roger Francois, Tom Weber, an anonymous referee, and GBC editor Katsumi Matsumoto. In addition, comments from Jess Adkins and two anonymous referees improved a previous version of this paper. Figure 1 was created using Ocean Data View (http://odv.awi.de/). Samples used in this study were provided by core repositories at the University of Rhode Island (TT013) and at the Lamont-Doherty Earth Observatory (VM and RC).

References

Anderson, D. M., & Archer, D. (2002). Glacial-interglacial stability of ocean pH inferred from foraminifer dissolution rates. *Nature*, *416*(6876), 70–73. https://doi.org/10.1038/416070a

Anderson, L. A. (1995). On the hydrogen and oxygen content of marine phytoplankton. *Deep-Sea Research Part I-Oceanographic Research Papers*, *42*(9), 1675–1680. https://doi.org/10.1016/0967-0637(95)00072-E

Anderson, R. F., Ali, S., Bradtmiller, L. I., Nielsen, S. H. H., Fleisher, M. Q., Anderson, B. E., & Burckle, L. H. (2009). Wind-driven upwelling in the Southern Ocean and the deglacial rise in atmospheric CO_2. *Science*, *323*(5920), 1443–1448. https://doi.org/10.1126/science.1167441

Anderson, R. F., Fleisher, M. Q., & Lao, Y. (2006). Glacial-interglacial variability in the delivery of dust to the central equatorial Pacific Ocean. *Earth and Planetary Science Letters*, *242*(3-4), 406–414. https://doi.org/10.1016/j.epsl.2005.11.061

Anderson, R. F., Fleisher, M. Q., Lao, Y., & Winckler, G. (2008). Modern $CaCO_3$ preservation in equatorial Pacific sediments in the context of recent glacial cycles. *Marine Chemistry*, *111*(1-2), 30–46. https://doi.org/10.1016/j.marchem.2007.11.011

Archer, D., & Maier-Reimer, E. (1994). Effect of deep-sea sedimentary calcite preservation on atmospheric CO_2 concentration. *Nature*, *367*(6460), 260–263. https://doi.org/10.1038/367260a0

Archer, D., Winguth, A., Lea, D., & Mahowald, N. (2000). What caused the glacial/interglacial atmospheric pCO_2 cycles? *Reviews of Geophysics*, *38*(2), 159–189. https://doi.org/10.1029/1999RG000066

Arndt, S., Jørgensen, B. B., LaRowe, D. E., Middelburg, J. J., Pancost, R. D., & Regnier, P. (2013). Quantifying the degradation of organic matter in marine sediments: A review and synthesis. *Earth-Science Reviews*, *123*, 53–86. https://doi.org/10.1016/j.earscirev.2013.02.008

Bova, S. C., Herbert, T., Rosenthal, Y., Kalansky, J., Altabet, M., Chazen, C., et al. (2015). Links between eastern equatorial Pacific stratification and atmospheric CO_2 rise during the last deglaciation. *Paleoceanography*, *30*, 1407–1424. https://doi.org/10.1002/2015PA002816

Boyd, P. W., & Trull, T. W. (2007). Understanding the export of biogenic particles in oceanic waters: Is there consensus? *Progress in Oceanography*, *72*(4), 276–312. https://doi.org/10.1016/j.pocean.2006.10.007

Boyle, E. A. (1988). The role of vertical chemical fractionation in controlling late Quaternary atmospheric carbon-dioxide. *Journal of Geophysical Research*, *93*(C12), 15,701–15,714. https://doi.org/10.1029/JC093iC12p15701

Boyle, E. A. (1990). Quaternary deep-water paleoceanography. *Science*, *249*(4971), 863–870. https://doi.org/10.1126/science.249.4971.863

Bradtmiller, L. I., Anderson, R. F., Fleisher, M. Q., & Burckle, L. H. (2006). Diatom productivity in the equatorial Pacific Ocean from the last glacial period to the present: A test of the silicic acid leakage hypothesis. *Paleoceanography*, *21*, PA4201. https://doi.org/10.1029/2006PA001282

Bradtmiller, L. I., Anderson, R. F., Sachs, J. P., & Fleisher, M. Q. (2010). A deeper respired carbon pool in the glacial equatorial Pacific Ocean. *Earth and Planetary Science Letters*, *299*(3–4), 417–425. https://doi.org/10.1016/j.epsl.2010.09.022

Broecker, W. S. (1982). Glacial to interglacial changes in ocean chemistry. *Progress in Oceanography*, *11*(2), 151–197. https://doi.org/10.1016/0079-6611(82)90007-6

Broecker, W. S., & Peng, T. H. (1974). Gas exchange rates between air and sea. *Tellus*, *26*(1-2), 21–35. https://doi.org/10.1111/j.2153-3490.1974.tb01948.x

Broecker, W. S., & Peng, T. H. (1987). The role of $CaCO_3$ compensation in the glacial to interglacial atmospheric CO_2 change. *Global Biogeochemical Cycles*, *1*(1), 15–29. https://doi.org/10.1029/GB001i001p00015

Broecker, W. S., & Sanyal, A. (1997). Magnitude of the $CaCO_3$ dissolution events marking the onset of times of glaciation. *Paleoceanography*, *12*(4), 530–532. https://doi.org/10.1029/97PA01020

Buesseler, K. O., Lamborg, C. H., Boyd, P. W., Lam, P. J., Trull, T. W., Bidigare, R. R., et al. (2007). Revisiting carbon flux through the ocean's twilight zone. *Science*, *316*(5824), 567–570. https://doi.org/10.1126/science.1137959

Burdige, D. J. (2007). Preservation of organic matter in marine sediments: Controls, mechanisms, and an imbalance in sediment organic carbon budgets? *Chemical Reviews*, *107*(2), 467–485. https://doi.org/10.1021/cr050347q

Chase, Z., Anderson, R. F., Fleisher, M. Q., & Kubik, P. (2003). Accumulation of biogenic and lithogenic material in the Pacific sector of the Southern Ocean during the past 40,000 years. *Deep Sea Research, Part II*, *50*(3-4), 799–832. https://doi.org/10.1016/S0967-0645(02)00595-7

Costa, K. M., Jacobel, A. W., McManus, J. F., Anderson, R. F., Winckler, G., & Thiagarajan, N. (2017). Productivity patterns in the equatorial Pacific over the last 30,000 years. *Global Biogeochemical Cycles*, *31*, 850–865. https://doi.org/10.1002/2016GB005579

Costa, K. M., & McManus, J. (2017). Efficacy of ^{230}Th normalization in sediments from the Juan de Fuca Ridge, northeast Pacific Ocean. *Geochimica et Cosmochimica Acta*, *197*, 215–225. https://doi.org/10.1016/j.gca.2016.10.034

Costa, K. M., McManus, J. F., Anderson, R. F., Ren, H., Sigman, D. M., Winckler, G., et al. (2016). No iron fertilization in the equatorial Pacific Ocean during the last ice age. *Nature*, *529*(7587), 519–522. https://doi.org/10.1038/nature16453

Cowie, G., Mowbray, S., Kurian, S., Sarkar, A., White, C., Anderson, A., Vergnaud, B., et al. (2014). Comparative organic geochemistry of Indian margin (Arabian Sea) sediments: Estuary to continental slope. *Biogeosciences*, *11*(23), 6683–6696. https://doi.org/10.5194/bg-11-6683-2014

de la Fuente, M., Calvo, E., Skinner, L., Pelejero, C., Evans, D., Müller, W., et al. (2017). The evolution of deep ocean chemistry and respired carbon in the eastern equatorial Pacific over the last deglaciation. *Paleoceanography*, *32*, 1371–1385. https://doi.org/10.1002/2017PA003155

Denton, G. H., Anderson, R. F., Toggweiler, J. R., Edwards, R. L., Schaefer, J. M., & Putnam, A. E. (2010). The last glacial termination. *Science*, *328*(5986), 1652–1656. https://doi.org/10.1126/science.1184119

DeVries, T. (2018). New directions for ocean nutrients. *Nature Geoscience*, *11*(1), 15–16. https://doi.org/10.1038/s41561-017-0042-z

DeVries, T., & Deutsch, C. (2014). Large-scale variations in the stoichiometry of marine organic matter respiration. *Nature Geoscience*, *7*(12), 890–894. https://doi.org/10.1038/ngeo2300

Dickson, A. G. (1990). Standard potential of the reaction: AgCl(s) + 1/2 H_2(g) = Ag(s) + HCl (aq), and the standard acidity constant of the ion HSO_4^- in synthetic seawater from 273.15 to 318.15 K. *Journal of Chemical Thermodynamics*, *22*(2), 113–127. https://doi.org/10.1016/0021-9614(90)90074-Z

Dickson, A. G., & Millero, F. J. (1987). A comparison of the equilibrium constants for the dissociation of carbonic acid in seawater media. *Deep-Sea Research*, *34*(10), 1733–1743. https://doi.org/10.1016/0198-0149(87)90021-5

Duteil, O., Koeve, W., Oschlies, A., Bianchi, D., Galbraith, E., Kriest, I., & Matear, R. (2013). A novel estimate of ocean oxygen utilisation points to a reduced rate of respiration in the ocean interior. *Biogeosciences*, *10*(11), 7723–7738. https://doi.org/10.5194/bg-10-7723-2013

Elderfield, H., Greaves, M., Barker, S., Hall, I. R., Tripati, A., Ferretti, P., et al. (2010). A record of bottom water temperature and seawater δ^{18}O for the Southern Ocean over the past 440 kyr based on Mg/Ca of benthic foraminiferal *Uvigerina* spp. *Quaternary Science Reviews*, *29*(1–2), 160–169. https://doi.org/10.1016/j.quascirev.2009.07.013

Fairbanks, R. G. (1989). A 17,000-year glacio-eustatic sea-level record—Influence of glacial melting rates on the Younger Dryas event and deep-ocean circulation. *Nature*, *342*(6250), 637–642. https://doi.org/10.1038/342637a0

Fleisher, M. Q., & Anderson, R. F. (2003). Assessing the collection efficiency of Ross Sea sediment traps using ^{230}Th and ^{231}Pa. *Deep-Sea Research Part II*, *50*(3-4), 693–712. https://doi.org/10.1016/S0967-0645(02)00591-X

Francois, R., Altabet, M. A., Yu, E. F., Sigman, D. M., Bacon, M. P., Frank, M., et al. (1997). Contribution of Southern Ocean surface-water stratification to low atmospheric CO_2 concentrations during the last glacial period. *Nature*, *389*(6654), 929–935. https://doi.org/10.1038/40073

Francois, R., Frank, M., Rutgers van der Loeff, M. M., & Bacon, M. P. (2004). Th-230 normalization: An essential tool for interpreting sedimentary fluxes during the late Quaternary. *Paleoceanography*, *19*, PA1018. https://doi.org/10.1029/2003PA000939

Francois, R., Frank, M., van der Loeff, M. R., Bacon, M. P., Geibert, W., Kienast, S., et al. (2007). Comment on "Do geochemical estimates of sediment focusing pass the sediment test in the equatorial Pacific?" by M. Lyle et al. *Paleoceanography*, *22*, PA1216. https://doi.org/10.1029/2005PA001235

Galbraith, E. D., & Jaccard, S. L. (2015). Deglacial weakening of the oceanic soft tissue pump: Global constraints from sedimentary nitrogen isotopes and oxygenation proxies. *Quaternary Science Reviews*, *109*, 38–48. https://doi.org/10.1016/j.quascirev.2014.11.012

Ganeshram, R. S., Francois, R., Commeau, J., & Brown-Leger, S. L. (2003). An experimental investigation of barite formation in seawater. *Geochimica et Cosmochimica Acta*, *67*(14), 2599–2605. https://doi.org/10.1016/S0016-7037(03)00164-9

Garcia, H. E., & Gordon, L. I. (1992). Oxygen solubility in seawater—Better fitting equations. *Limnology and Oceanography*, *37*(6), 1307–1312. https://doi.org/10.4319/lo.1992.37.6.1307

Garcia, H. E., Locarnini, R. A., Boyer, T. P., Antonov, J. I., Baranova, O. K., Zweng, M. M., & Johnson, D. R. (2010). *World ocean atlas 2009, Volume 3: Dissolved oxygen, apparent oxygen utilization, and oxygen saturation*. Washington, D. C: U. S. Government Printint Office.

Gordon, A. L., & Huber, B. A. (1990). Southern Ocean winter mixed layer. *Journal of Geophysical Research*, *95*(C7), 11,655–11,672. https://doi.org/10.1029/JC095iC07p11655

Gordon, A. L., Visbeck, M., & Huber, B. (2001). Export of Weddell Sea deep and bottom water. *Journal of Geophysical Research*, *106*(C5), 9005–9017. https://doi.org/10.1029/2000JC000281

Gottschalk, J., Skinner, L. C., Lippold, J., Vogel, H., Frank, N., Jaccard, S. L., & Waelbroeck, C. (2016). Biological and physical controls in the Southern Ocean on past millennial-scale atmospheric CO_2 changes. *Nature Communications*, *7*(1). https://doi.org/10.1038/ncomms11539

Gottschalk, J., Vázquez Riveiros, N., Waelbroeck, C., Skinner, L. C., Michel, E., Duplessy, J.-C., et al. (2016). Carbon isotope offsets between benthic foraminifer species of the genus *Cibicides* (Cibicidoides) in the glacial sub-Antarctic Atlantic. *Paleoceanography*, *31*, 1583–1602. https://doi.org/10.1002/2016PA003029

Hain, M. P., Sigman, D. M., & Haug, G. H. (2010). Carbon dioxide effects of Antarctic stratification, North Atlantic Intermediate Water formation, and subantarctic nutrient drawdown during the last ice age: Diagnosis and synthesis in a geochemical box model. *Global Biogeochemical Cycles*, *24*, GB4023. https://doi.org/10.1029/2010GB003790

Hall, I. R., McCave, I. N., Shackleton, N. J., Weedon, G. P., & Harris, S. E. (2001). Intensified deep Pacfic inflow and ventilation in Pleistocene glacial times. *Nature*, *412*(6849), 809–812. https://doi.org/10.1038/35090552

Hartnett, H. E., Keil, R. G., Hedges, J. I., & Devol, A. H. (1998). Influence of oxygen exposure time on organic carbon preservation in continental margin sediments. *Nature*, *391*(6667), 572–575. https://doi.org/10.1038/35351

Hayes, C. T., Anderson, R. F., & Fleisher, M. Q. (2011). Opal accumulation rates in the equatorial Pacific and mechanisms of deglaciation. *Paleoceanography*, *26*, PA1207. https://doi.org/10.1029/2010PA002008

Hernandez-Sanchez, M. T., Mills, R. A., Planquette, H., Pancost, R. D., Hepburn, L., Salter, I., & FitzGeorge-Balfour, T. (2011). Quantifying export production in the Southern Ocean: Implications for the Ba_{xs} proxy. *Paleoceanography*, *26*, PA4222. https://doi.org/10.1029/2010PA002111

Honisch, B., Hemming, N. G., Archer, D., Siddall, M., & McManus, J. F. (2009). Atmospheric carbon dioxide concentration across the mid-Pleistocene transition. *Science*, *324*(5934), 1551–1554. https://doi.org/10.1126/science.1171477

Hoogakker, B. A. A., Elderfield, H., Schmiedl, G., McCave, I. N., & Rickaby, R. E. M. (2015). Glacial-interglacial changes in bottom-water oxygen content on the Portuguese margin. *Nature Geoscience*, *8*(1), 40–43. https://doi.org/10.1038/ngeo2317

Hoogakker, B. A. A., Lu, Z., Umling, N., Jones, L., Zhou, X., Rickaby, R. E. M., et al. (2018). Glacial expansion of oxygen-depleted seawater in the eastern tropical Pacific. *Nature*, *562*(7727), 410–413. https://doi.org/10.1038/s41586-018-0589-x

Ito, T., & Follows, M. J. (2013). Air-sea disequilibrium of carbon dioxide enhances the biological carbon sequestration in the Southern Ocean. *Global Biogeochemical Cycles*, *27*, 1129–1138. https://doi.org/10.1002/2013GB004682

Ito, T., Follows, M. J., & Boyle, E. A. (2004). Is AOU a good measure of respiration in the oceans? *Geophysical Research Letters*, *31*, L17305. https://doi.org/10.1029/2004GL020900

Jaccard, S. L., & Galbraith, E. D. (2012). Large climate-driven changes of oceanic oxygen concentrations during the last deglaciation. *Nature Geoscience*, *5*(2), 151–156. https://doi.org/10.1038/ngeo1352

Jaccard, S. L., Galbraith, E. D., Frölicher, T. L., & Gruber, N. (2014). Ocean (de)oxygenation across the last deglaciation. *Oceanography*, *27*(1), 26–35. https://doi.org/10.5670/oceanog.2014.05

Jaccard, S. L., Galbraith, E. D., Martínez-García, A., & Anderson, R. F. (2016). Covariation of deep Southern Ocean oxygenation and atmospheric CO_2 through the last ice age. *Nature*, *530*(7589), 207–210. https://doi.org/10.1038/nature16514

Jaccard, S. L., Galbraith, E. D., Sigman, D. M., Haug, G. H., Francois, R., Pedersen, T. F., et al. (2009). Subarctic Pacific evidence for a glacial deepening of the oceanic respired carbon pool. *Earth and Planetary Science Letters*, *277*(1–2), 156–165. https://doi.org/10.1016/j.epsl.2008.10.017

Keil, R. G., & Cowie, G. L. (1999). Organic matter preservation through the oxygen-deficient zone of the NE Arabian Sea as discerned by organic carbon: Mineral surface area ratios. *Marine Geology*, *161*(1), 13–22. https://doi.org/10.1016/S0025-3227(99)00052-3

Kobayashi, H., & Oka, A. (2018). Response of atmospheric pCO_2 to glacial changes in the Southern Ocean amplified by carbonate compensation. *Paleoceanography and Paleoclimatology*, *33*, 1206–1229. https://doi.org/10.1029/2018PA003360

Koho, K. A., Nierop, K. G. J., Moodley, L., Middelburg, J. J., Pozzato, L., Soetaert, K., et al. (2013). Microbial bioavailability regulates organic matter preservation in marine sediments. *Biogeosciences*, *10*(2), 1131–1141. https://doi.org/10.5194/bg-10-1131-2013

Korff, L., von Dobeneck, T., Frederichs, T., Kasten, S., Kuhn, G., Gersonde, R., & Diekmann, B. (2016). Cyclic magnetite dissolution in Pleistocene sediments of the abyssal Northwest Pacific Ocean: Evidence for glacial oxygen depletion and carbon trapping. *Paleoceanography*, *31*, 600–624. https://doi.org/10.1002/2015PA002882

Koutavas, A., & Lynch-Stieglitz, J. (2003). Glacial-interglacial dynamics of the eastern equatorial Pacific cold tongue Intertropical Convergence Zone system reconstructed from oxygen isotope records. *Paleoceanography*, *18*(4), 1089. https://doi.org/10.1029/2003PA000894

Koutavas, A., & Sachs, J. P. (2008). Northern timing of deglaciation in the eastern equatorial Pacific from alkenone paleothermometry. *Paleoceanography*, *23*, PA4205. https://doi.org/10.1029/2008PA001593

Lao, Y., Anderson, R. F., Broecker, W. S., Hofmann, H. J., & Wolfli, W. (1993). Particulate fluxes of ^{230}Th, ^{231}Pa and ^{10}Be in the northeastern Pacific Ocean. *Geochimica et Cosmochimica Acta*, *57*(1), 205–217. https://doi.org/10.1016/0016-7037(93)90479-G

Lengger, S. K., Hopmans, E. C., Sinninghe Damsté, J. S., & Schouten, S. (2014). Impact of sedimentary degradation and deep water column production on GDGT abundance and distribution in surface sediments in the Arabian Sea: Implications for the TEX86 paleothermometer. *Geochimica et Cosmochimica Acta*, *142*, 386–399. https://doi.org/10.1016/j.gca.2014.07.013

Loubere, P. (1999). A multiproxy reconstruction of biological productivity and oceanography in the eastern equatorial Pacific for the past 30,000 years. *Marine Micropaleontology*, *37*(2), 173–198. https://doi.org/10.1016/S0377-8398(99)00013-4

Lu, Z., Hoogakker, B. A. A., Hillenbrand, C.-D., Zhou, X., Thomas, E., Gutchess, K. M., et al. (2016). Oxygen depletion recorded in upper waters of the glacial Southern Ocean. *Nature Communications*, *7*(1), 7. https://doi.org/10.1038/ncomms11146

Lüthi, D., Le Floch, M., Bereiter, B., Blunier, T., Barnola, J.-M., Siegenthaler, U., et al. (2008). High-resolution carbon dioxide concentration record 650,000–800,000 years before present. *Nature*, *453*(7193), 379–382. https://doi.org/10.1038/nature06949

Lyle, M. (1988). Climatically forced organic-carbon burial in equatorial Atlantic and Pacific Oceans. *Nature*, *335*(6190), 529–532. https://doi.org/10.1038/335529a0

Lyle, M., Marcantonio, F., Moore, W. S., Murray, R. W., Huh, C.-A., Finney, B. P., et al. (2014). Sediment size fractionation and focusing in the equatorial Pacific: Effect on ^{230}Th normalization and paleoflux measurements. *Paleoceanography*, *29*, 747–763. https://doi.org/10.1002/2014PA002616

Lyle, M., Mix, A., & Pisias, N. (2002). Patterns of $CaCO_3$ deposition in the eastern tropical Pacific Ocean for the last 150 kyr: Evidence for a southeast Pacific depositional spike during marine isotope stage (MIS) 2. *Paleoceanography*, *17*(2), 1013. https://doi.org/10.1029/2000PA000538

Lyle, M., Murray, D. W., Finney, B. P., Dymond, J., Robbins, J. M., & Brooksforce, K. (1988). The record of Late Pleistocene biogenic sedimentation in the eastern tropical Pacific Ocean. *Paleoceanography*, *3*(1), 39–59. https://doi.org/10.1029/PA003i001p00039

Mangini, A., Eisenhauer, A., & Walter, P. (1990). Response of manganese in the ocean to the climatic cycles in the Quaternary. *Paleoceanography*, *5*(5), 811–821. https://doi.org/10.1029/PA005i005p00811

Martin, J. H., Knauer, G. A., Karl, D. M., & Broenkow, W. W. (1987). VERTEX—Carbon cycling in the Northeast Pacific. *Deep-Sea Research Part A-Oceanographic Research Papers*, *34*(2), 267–285. https://doi.org/10.1016/0198-0149(87)90086-0

Martinez-Boti, M. A., Marino, G., Foster, G. L., Ziveri, P., Henehan, M. J., Rae, J. W. B., et al. (2015). Boron isotope evidence for oceanic carbon dioxide leakage during the last deglaciation. *Nature*, *518*(7538), 219–222. https://doi.org/10.1038/nature14155

Martinson, D. G., Pisias, N. G., Hays, J. D., Imbrie, J., Moore, T. C., & Shackleton, N. J. (1987). Age dating and the orbital theory of the ice ages—Development of a high-resolution 0 to 300,000-year chronostratigraphy. *Quaternary Research*, *27*(01), 1–29. https://doi.org/10.1016/0033-5894(87)90046-9

Martiny, A. C., Pham, C. T. A., Primeau, F. W., Vrugt, J. A., Moore, J. K., Levin, S. A., & Lomas, M. W. (2013). Strong latitudinal patterns in the elemental ratios of marine plankton and organic matter. *Nature Geoscience*, *6*(4), 279–283. https://doi.org/10.1038/ngeo1757

Martiny, A. C., Vrugt, J. A., Primeau, F. W., & Lomas, M. W. (2013). Regional variation in the particulate organic carbon to nitrogen ratio in the surface ocean. *Global Biogeochemical Cycles*, *27*, 723–731. https://doi.org/10.1002/gbc.20061

Mehrbach, C., Culberson, C. H., Hawley, J. E., & Pytkowicz, R. M. (1973). Measurement of the apparent dissociation constants of carbonic acid in seawater at atmospheric pressure. *Limnology and Oceanography*, *18*(6), 897–907. https://doi.org/10.4319/lo.1973.18.6.0897

Mills, R. A., Taylor, S. L., Pälike, H., & Thomson, J. (2010). Hydrothermal sediments record changes in deep water oxygen content in the SE Pacific. *Paleoceanography*, *25*, PA4226. https://doi.org/10.1029/2010PA001959

Mitchell, N. C., & Huthnance, J. M. (2013). Geomorphological and geochemical evidence (^{230}Th anomalies) for cross-equatorial currents in the central Pacific. *Deep Sea Research Part I: Oceanographic Research Papers*, *78*, 24–41. https://doi.org/10.1016/j.dsr.2013.04.003

Mix, A. C., Pisias, N. G., Rugh, W., Wilson, J., Morey, A., & Hagelberg, T. (1995). Benthic foraminiferal stable isotope record from Site 849, 0–5 Ma: Local and global climate changes. *Proceeding of the Ocean Drilling Program, Scientific Results*, *138*, 371–412.

Mortlock, R. A., & Froelich, P. N. (1989). A simple method for the rapid-determination of biogenic opal in pelagic marine-sediments. *Deep-Sea Research Part A-Oceanographic Research Papers*, *36*(9), 1415–1426. https://doi.org/10.1016/0198-0149(89)90092-7

Murray, R. W., Knowlton, C., Leinen, M., Mix, A. C., & Polsky, C. H. (2000). Export production and carbonate dissolution in the central equatorial Pacific Ocean over the past 1 Myr. *Paleoceanography*, *15*(6), 570–592. https://doi.org/10.1029/1999PA000457

Murray, R. W., Leinen, M., & Knowlton, C. W. (2012). Links between iron input and opal deposition in the Pleistocene equatorial Pacific Ocean. *Nature Geoscience*, *5*(4), 270–274. https://doi.org/10.1038/ngeo1422

Omta, A. W., Ferrari, R., & McGee, D. (2018). An analytical framework for the steady state impact of carbonate compensation on atmospheric CO_2. *Global Biogeochemical Cycles*, *32*, 720–735. https://doi.org/10.1002/2017GB005809

Palmer, M. R., & Pearson, P. N. (2003). A 23,000-year record of surface water pH and pCO_2 in the western equatorial Pacific Ocean. *Science*, *300*(5618), 480–482. https://doi.org/10.1126/science.1080796

Pedersen, T. F. (1983). Increased productivity in the eastern equatorial Pacific during the Last Glacial Maximum (19,000 to 14,000 Yr BP). *Geology*, *11*(1), 16–19. https://doi.org/10.1130/0091-7613(1983)11<16:IPITEE>2.0.CO;2

Perks, H. M., Charles, C. D., & Keeling, R. F. (2002). Precessionally forced productivity variations across the equatorial Pacific. *Paleoceanography*, *17*(3), 1037. https://doi.org/10.1029/2000PA000603

Perks, H. M., & Keeling, R. F. (1998). A 400 kyr record of combustion oxygen demand in the western equatorial Pacific: Evidence for a precessionally forced climate response. *Paleoceanography*, *13*(1), 63–69. https://doi.org/10.1029/97PA02892

Peterson, C. D., & Lisiecki, L. E. (2018). Deglacial carbon cycle changes observed in a compilation of 127 benthic δ^{13}C time series (20–6 ka). *Climate of the Past*, *14*(8), 1229–1252. https://doi.org/10.5194/cp-14-1229-2018

Peterson, C. D., Lisiecki, L. E., & Stern, J. V. (2014). Deglacial whole-ocean δ^{13}C change estimated from 480 benthic foraminiferal records. *Paleoceanography*, *29*, 549–563. https://doi.org/10.1002/2013PA002552

Prahl, F. G., Muehlhausen, L. A., & Lyle, M. (1989). An organic geochemical assessment of oceanographic conditions at MANOP site C over the past 26,000 years. *Paleoceanography*, *4*(5), 495–510. https://doi.org/10.1029/PA004i005p00495

Rae, J. W. B., Burke, A., Robinson, L. F., Adkins, J. F., Chen, T., Cole, C., et al. (2018). CO_2 storage and release in the deep Southern Ocean on millennial to centennial timescales. *Nature*, *562*(7728), 569–573. https://doi.org/10.1038/s41586-018-0614-0

Rampen, S. W., Abbas, B. A., Schouten, S., & Damste, J. S. S. (2010). A comprehensive study of sterols in marine diatoms (Bacillariophyta): Implications for their use as tracers for diatom productivity. *Limnology and Oceanography*, *55*(1), 91–105. https://doi.org/10.4319/lo.2010.55.1.0091

Redfield, A. C. (1958). The biological control of chemical factors in the environment. *American Scientist*, *46*(3), 205–221.

Riedinger, N., Kasten, S., Gröger, J., Franke, C., & Pfeifer, K. (2006). Active and buried authigenic barite fronts in sediments from the eastern Cape Basin. *Earth and Planetary Science Letters*, *241*(3-4), 876–887. https://doi.org/10.1016/j.epsl.2005.10.032

Rodrigo-Gámiz, M., Rampen, S. W., Schouten, S., & Sinninghe Damsté, J. S. (2016). The impact of oxic degradation on long chain alkyl diol distributions in Arabian Sea surface sediments. *Organic Geochemistry*, *100*, 1–9. https://doi.org/10.1016/j.orggeochem.2016.07.003

Rudnick, R. L., & Gao, R. (2003). Composition of the continental crust. In R. Rudnick (Ed.), *The crust, vol 3 treatise on geochemistry* (pp. 1–64). Oxford: Elsevier-Pergamon. https://doi.org/10.1016/B0-08-043751-6/03016-4

Sachs, J. P., & Anderson, R. F. (2003). Fidelity of alkenone paleotemperatures in southern Cape Basin sediment drifts. *Paleoceanography*, *18*(4), 1082. https://doi.org/10.1029/2002PA000862

Sarmiento, J. L., & Gruber, N. (2006). *Global biogeochemical dynamics*. Princeton, NJ: Princeton University Press.

Sarnthein, M., Schneider, B., & Grootes, P. M. (2013). Peak glacial ^{14}C ventilation ages suggest major draw-down of carbon into the abyssal ocean. *Climate of the Past*, *9*(6), 2595–2614. https://doi.org/10.5194/cp-9-2595-2013

Sarnthein, M., Winn, K., Duplessy, J. C., & Fontugne, M. R. (1988). Global variations of surface ocean productivity in low and mid latitudes: Influence on CO_2 reservoirs of the deep ocean and atmospheric during the last 21,000 years. *Paleoceanography*, *3*(3), 361–399. https://doi.org/10.1029/PA003i003p00361

Sayles, F. L., Martin, W. R., Chase, Z., & Anderson, R. F. (2001). Benthic remineralization and burial of biogenic SiO_2, $CaCO_3$, organic carbon and detrital material in the Southern Ocean along a transect at 170° west. *Deep Sea Research, Part II*, *48*(19-20), 4323–4383. https://doi.org/10.1016/S0967-0645(01)00091-1

Schmittner, A., & Somes, C. J. (2016). Complementary constraints from carbon (^{13}C) and nitrogen (^{15}N) isotopes on the glacial ocean's soft-tissue biological pump. *Paleoceanography*, *31*, 669–693. https://doi.org/10.1002/2015PA002905

Shackleton, N. J., Imbrie, J., & Hall, M. A. (1983). Oxygen and carbon isotope record of East Pacific core V19-30—Implications for the formation of deep-water in the Late Pleistocene North-Atlantic. *Earth and Planetary Science Letters*, *65*(2), 233–244. https://doi.org/10.1016/0012-821X(83)90162-0

Sigman, D. M., & Boyle, E. A. (2000). Glacial/interglacial variations in atmospheric carbon dioxide. *Nature*, *407*(6806), 859–869. https://doi.org/10.1038/35038000

Sigman, D. M., Hain, M. P., & Haug, G. H. (2010). The polar ocean and glacial cycles in atmospheric CO_2 concentration. *Nature*, *466*(7302), 47–55. https://doi.org/10.1038/nature09149

Singh, A. K., Marcantonio, F., & Lyle, M. (2013). Water column ^{230}Th systematics in the eastern equatorial Pacific Ocean and implications for sediment focusing. *Earth and Planetary Science Letters*, *362*, 294–304. https://doi.org/10.1016/j.epsl.2012.12.006

Sinninghe Damste, J. S., Rijpstra, W. I. C., & Reichart, G. J. (2002). The influence of oxic degradation on the sedimentary biomarker record II. Evidence from Arabian Sea sediments. *Geochimica et Cosmochimica Acta*, *66*(15), 2737–2754. https://doi.org/10.1016/S0016-7037(02)00865-7

Skinner, L., McCave, I. N., Carter, L., Fallon, S., Scrivner, A. E., & Primeau, F. (2015). Reduced ventilation and enhanced magnitude of the deep Pacific carbon pool during the last glacial period. *Earth and Planetary Science Letters*, *411*, 45–52. https://doi.org/10.1016/j.epsl.2014.11.024

Skinner, L. C., Primeau, F., Freeman, E., de la Fuente, M., Goodwin, P. A., Gottschalk, J., et al. (2017). Radiocarbon constraints on the glacial ocean circulation and its impact on atmospheric CO_2. *Nature Communications*, *8*, 16010. https://doi.org/10.1038/ncomms16010

Stephens, B. B., & Keeling, R. F. (2000). The influence of Antarctic Sea ice on glacial-interglacial CO_2 variations. *Nature*, *404*(6774), 171–174. https://doi.org/10.1038/35004556

Talarmin, A., Lomas, M. W., Bozec, Y., Savoye, N., Frigstad, H., Karl, D. M., & Martiny, A. C. (2016). Seasonal and long-term changes in elemental concentrations and ratios of marine particulate organic matter. *Global Biogeochemical Cycles*, *30*, 1699–1711. https://doi.org/10.1002/2016GB005409

Tanioka, T., & Matsumoto, K. (2017). Buffering of ocean export production by flexible elemental stoichiometry of particulate organic matter. *Global Biogeochemical Cycles*, *31*, 1528–1542. https://doi.org/10.1002/2017GB005670

Torres, M. E., Brumsack, H. J., Bohrmann, G., & Emeis, K. C. (1996). Barite fronts in continental margin sediments: A new look at barium remobilization in the zone of sulfate reduction and formation of heavy barites in diagenetic fronts. *Chemical Geology*, *127*(1–3), 125–139. https://doi.org/10.1016/0009-2541(95)00090-9

Umling, N. E., & Thunell, R. C. (2018). Mid-depth respired carbon storage and oxygenation of the eastern equatorial Pacific over the last 25,000 years. *Quaternary Science Reviews*, *189*, 43–56. https://doi.org/10.1016/j.quascirev.2018.04.002

Uppstrom, L. R. (1974). The boron/chloronity ratio of deep-sea water from the Pacific Ocean. *Deep-Sea Research*, *21*, 161–162.

Volkman, J. K., Barrett, S. M., Blackburn, S. I., Mansour, M. P., Sikes, E. L., & Gelin, F. (1998). Microalgal biomarkers: A review of recent research developments. *Organic Geochemistry*, *29*(5–7), 1163–1179. https://doi.org/10.1016/S0146-6380(98)00062-X

Winckler, G., Anderson, R. F., Jaccard, S. L., & Marcantonio, F. (2016). Ocean dynamics, not dust, have controlled equatorial Pacific productivity over the past 500,000 years. *Proceedings of the National Academy of Sciences*, *113*(22), 6119–6124. https://doi.org/10.1073/pnas.1600616113

Yu, J., Anderson, R. F., Jin, Z., Rae, J. W. B., Opdyke, B. N., & Eggins, S. M. (2013). Responses of the deep ocean carbonate system to carbon reorganization during the last glacial–interglacial cycle. *Quaternary Science Reviews*, *76*, 39–52. https://doi.org/10.1016/j.quascirev.2013.06.020